In-Process Ultrasonic Inspection of S275 Steel GTAW Butt Welds Through Non-Contact Ultrasonic Guided Waves

Momchil Vasilev, Charles MacLeod, Walter Galbraith, Yashar Javadi, Euan Foster, Gordon Dobie, Gareth Pierce, Anthony Gachagan

***Abstract*— Joining of metal structures or welding, has an important role in our modern world, with safety critical welds of thin sheet metals being widely used in airplane fuselages, boilers and nuclear cannisters among others. A potential failure in such welds could prove to be catastrophic, hence the need for thorough inspection and testing. With the ever-increasing automation of welding operations, manually deployed Non-destructive Evaluation (NDE) has become a major bottleneck in the supply chain. This paper presents a weld inspection approach deployed at the point of manufacture using non-contact air-coupled ultrasonic transducers deploying surface guided Lamb waves. Advantages of the outlined method include higher production rates, reduced levels of scrap and higher production quality in regards to thin metal sheet welded components. 3mm thick mild steel plates are butt welded together using Gas Tungsten Arc Welding (GTAW) while a continuous ultrasonic inspection is performed on a section of the weld seam. By performing multiple trials at varying levels of welding input power, it is demonstrated that the amplitude of through transmission A0 Lamb wave is correlated to weld geometry and can be used for on-line weld quality screening.**

***Index Terms*— Guided waves, In-process inspection, Nondestructive evaluation (NDE), Welding**

I. Introduction

A. Justification

JOINING of metallic structures or welding, is an important part of our modern world, being employed in numerous high-value manufacturing industries. Many of the welded joints serve a key structural and safety role and hence their integrity is paramount. Safety critical welds in thin sheet metals are used in sectors where space and light-weighting is essential, such as in airplane fuselages, low-pressure boilers, pipework and nuclear storage cannisters. These welds are required to be thoroughly tested to ensure their safety and integrity, as a potential failure of these could be catastrophic. Non-destructive evaluation (NDE) allows for such welds to be tested unobtrusively, without the need of cutting or damaging them during the inspection process, and is for that reason widely utilised in practice. Ultrasonic Testing (UT) is the preferred technique used for welded components due to its ability to detect and size both planar and volumetric defects [1].

In the dawn of Industry 4.0 [2] sensor enabled robotic applications offer commercial and technical advantages in terms of quality and production efficiency of final product [3], [4]. With an increasing number of high-value welding operations automated through the use of articulated robots, NDE has become a major bottleneck in the production process, as it is traditionally manually deployed post manufacture. Therefore, inspection at the point of manufacture, also known as in-process or on-line inspection, is sought after and brings forward many advantages over manual deployment such as, higher production rates, lower quantities of scrap and higher overall quality. The opportunity also exists not only to detect but also to repair weld flaws in-process as they develop using advanced imaging and fast low-latency control.

B. Welding

Fusion welding is a permanent joining method, where two solids are fused by a moving liquid weld pool [5]. A localised heat source lies at the heart of all welding processes as the workpiece needs to be heated up beyond its melting point (around 1500°C for mild steel) for fusion to occur. This could be induced using a high powered laser beam [6], a plasma arc, an electric arc or through mechanical friction. In Gas Tungsten Arc Welding (GTAW) a non-consumable Tungsten electrode maintains an electric arc to the workpiece and creates a localised melt pool. A consumable wire, usually from the same material as the workpiece, is added to the melt pool for joint reinforcement [7]. Protection from oxidation is provided through a shielding Argon gas coming/injected from the welding torch. There are many important parameters that

This paragraph of the first footnote will contain the date on which you submitted your paper for review. It will also contain support information, including sponsor and financial support acknowledgment. For example, "This work was supported in part by the U.S. Department of Commerce under Grant BS123456."

The next few paragraphs should contain the authors' current affiliations, including current address and e-mail. For example, F. A. Author is with the National Institute of Standards and Technology, Boulder, CO 80305 USA (e-mail: author@ boulder.nist.gov).

S. B. Author, Jr., was with Rice University, Houston, TX 77005 USA. He is now with the Department of Physics, Colorado State University, Fort Collins, CO 80523 USA (e-mail: author@lamar.colostate.edu).

T. C. Author is with the Electrical Engineering Department, University of Colorado, Boulder, CO 80309 USA, on leave from the National Research Institute for Metals, Tsukuba, Japan (e-mail: author@nrim.go.jp).

influence the overall quality of a weld, therefore in an attempt to simplify this, a universal measure for welding power has been adopted.

The arc energy measures how much energy has been supplied by the welding arc to the workpiece by taking into account the welding current, welding voltage and torch travel speed and is calculated from (1) [8].

$$AE = \frac{60 * V * I}{1000 * v} \quad (1)$$

AE Arc energy [kJ/mm]
V Welding voltage [V]
I Welding current [A]
v Travel speed [mm/min]

The heat input can also be calculated from the arc energy by including the efficiency of the specific welding process, but is not used here as all welds are created using the same process.

C. On-line NDE And Process Control

Ultrasonic waves are sound waves with a frequency above 20 kHz and are used in many industrial applications. Ultrasonic sensors are commonly associated with the automotive industry for their use in reverse obstacle detection and parking assist [9], operating at low frequencies e.g. 40 kHz [10]. In contrast, the frequency of ultrasonic sensors used for NDE is dictated by its wavelength in the material being examined, and the size of the expected defects. For example, 5 MHz ultrasonic wave would have a wavelength of approximately 1mm in steel.

Attempts have been made to incorporate NDE and other welding measurement approaches to improve the resultant joints and process control. Hyperspectral cameras were used during the welding process to identify welding current variations, protection gas shortages and changes in torch offset, however the developed system does not inspect the deposited weld [11]. Passive and active imaging respectively can be applied to monitor the weld pool and predict the weld bead geometry as shown in [12] and [13], but as they use visual sensors only surface flaws could be detected. A system for inspecting partially filled welds using Electromagnetic Acoustic Transducers (EMATs) utilising surface waves was introduced in [14]. Although implementing a non-contact UT method this was only demonstrated to work off-line after the welding passes were completed.

Conventional UT requires that the transducer and material under test are in direct contact, with a thin layer of liquid couplant between the two, facilitating the transmission of sound waves [15]. This is effective for inspection of as-built components, however introducing such liquid compounds to a workpiece during welding could produce many flaws like porosity, lack of fusion and slag inclusion among others. Therefore a non-contact NDE approach that requires no couplant would be preferable for in-process inspection. Furthermore, such couplants have high thermal conductivity which would enable heat transfer from a hot workpiece to the transducer. Traditional commercial contact high-temperature wedges allow transducers to only resist up to 150°C for very short periods of time [16] making in-process inspection

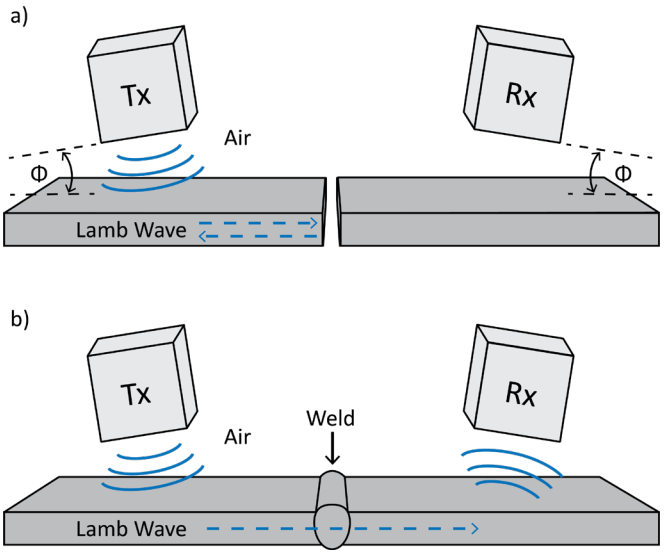

Fig. 1. Side view schematic of a non-contact air-coupled ultrasonic inspection of thin plates using guided Lamb waves. The transmitter and receiver are fixed at the specific angle Φ, calculated through the dispersion curves for the material of the specimen. a) Prior to welding the plates together, no all ultrasonic waves are internally reflected at the weld seam; b) after joining the ultrasonic Lamb waves propagate through the welded joint and are received by the receiving transducer.

impractical, whereas traditional probes can only accommodate up to 60°C [16]. Another key challenge of in-situ welding inspection is the large amount electromagnetic interference (EMI), which is radiated from the high frequency switching of the arc welder power source [17].

Given the outlined challenges of in-process weld inspection, non-contact ultrasonic testing proves to be favourable. Laser Ultrasonic (LU) systems generate soundwaves through the impact of photons on the test surface using pulsed laser beams and can be used to detect defects in thin metal sheets [18]. However, such high power laser systems are currently far more expensive than conventional UT systems and are cumbersome to implement, due to the beam enclosures and other health and safety measures that are required to be in place [19]. Non-contact gas-coupled UT on the other hand is rather inexpensive to implement, using air as the coupling medium between the transducer and test piece to transmit the sound waves as shown in Figure 1. There is, of course, a distinct disadvantage to such a concept, as due to the acoustic impedance mismatch, air is not as efficient as liquid couplants. The result is an expected 140dB reduction in signal amplitude, when comparing air-coupled to traditional contact based UT methods [15].

This paper presents a novel in-process inspection approach for testing thin-plate (3 mm) mild steel GTAW butt welds using non-contact air-coupled ultrasonic transducers. A total of seven samples were created using different welding parameters in order to test the sensitivity of the proposed approach. The method developed here is suitable for testing other metals such as Stainless Steel and Aluminium and can be applied to different welding processes such as Gas Metal Arc Welding (GMAW), and Plasma Arc Welding (PAW).

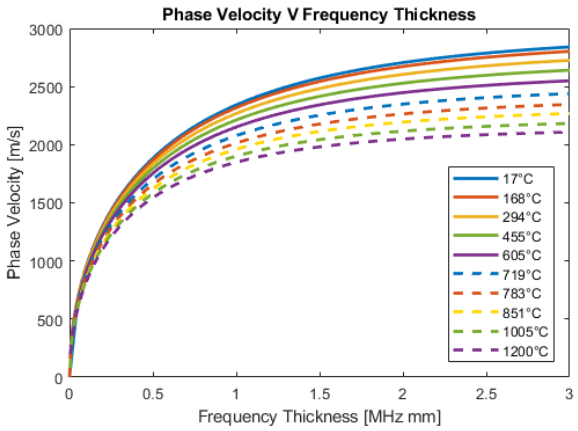

Fig. 2. Zeroth order asymmetric Lamb wave dispersion curves for S275 mild steel. Different lines represent the A0 curve in the temperature range 17°C to 1200°C.

II. NDE Using Ultrasonic Guided Waves

Guided waves have been used since the 1980s to inspect composite structures [20], [21] and are currently also employed in Structural Health Monitoring (SHM) and NDE for oil and gas pipelines [22], [23] , railway tracks [24] and remote structural inspection platforms [25]. Lamb waves are guided ultrasonic plate waves which are made up of longitudinal and transverse waves and can detect discontinuities and flaws inside the material under test. As transverse waves can only propagate in solid media, Lamb waves can also only propagate through solids. Their nature is such that encountering a flaw in the specimen would result in reflection and scattering, reducing the amplitude of the signal propagating across to the receiving transducer. Therefore, by monitoring the amplitude of the received Lamb waves it is possible to detect any potential flaws in the test specimen. The proposed inspection approach could be used in-process as a screening tool to aid process control and thus provide an early indication of any flaws developing in the welded joint.

Dispersion curves provide the phase velocity of the possible guided wave modes that can be excited in a material as a function of the Frequency-Thickness Product (FTP). The FTP, as the name suggests, is equal to the ultrasonic frequency multiplied by the thickness of the plate under test. The zeroth order asymmetric guided Lamb wave mode (A0) was selected, as it is suitable for generation by air-coupled transducers [26]. To do so, the air-coupled transducers have to be accurately set at an angle of incidence calculated using the phase velocity of the guided wave and the velocity of the incident wave in air (2) [15].

$$\sin(\Phi) = \frac{V_i}{V} \quad (2)$$

Φ Angle of incidence [°]
V_i Phase velocity of induced Lamb wave mode [m/s]
V Velocity of incident ultrasonic wave in air [m/s]

Figure 2 shows the phase velocity of the A0 mode in S275 mild steel as a function of the frequency-thickness product for a range of temperatures between 17°C and 1200°C, a suitable range of temperatures being encountered in fusion welding applications. The curves were calculated via the Disperse software package developed at Imperial College London [27] using experimentally acquired measurements of the velocity of sound in S275 mild steel at the different temperatures [28]. The results demonstrate that an increase in temperature of the workpiece would lead to a reduction of the propagation velocity of sound in the material and hence the optimal angle of incidence would be modified. An additional layer of complexity is added by the non-uniform temperature of the workpiece, inherently introduced by the welding process. As the effects of these temperature gradients on the Lamb wave propagation are yet to be explored, a decision was made to optimise the set-up using dispersion curves for the material at room temperature.

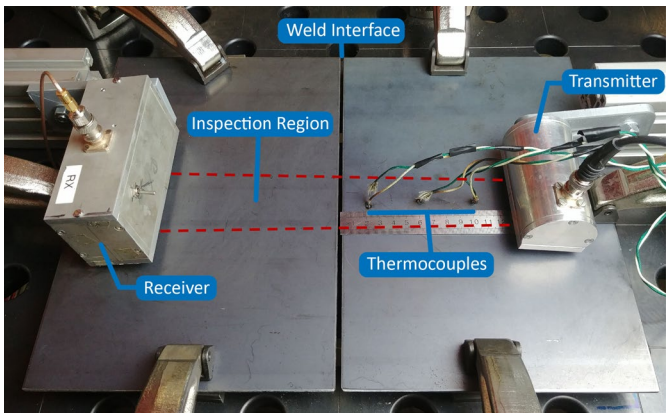

Fig. 3. In-process non-contact ultrasonic inspection set-up; the transmitting and receiving transducers are located on either side of the weld interface with the inspection region shown between the dashed lines; the three permanently welded thermocouples are located in the inspection region at a distance of 20mm, 60mm and 100mm from the weld interface.

III. Experimental Set-Up

A. Ultrasonic Method

Two ultrasonic non-contact 1-3 piezocomposite transducers [29] with a 30x30 mm element size and a 510 kHz centre frequency are laterally positioned on either side of the weld seam in a pitch catch arrangement, as shown in Figure 3. To maximise the amount of energy transmitted into the gas coupling medium, the transducers are fitted with a matching layer made up of silicone rubber and semiporous membrane as outlined in [30]. The plate thickness and transducer frequency used in the experiment provide an FTP of 1.53 Mhz.mm, which according to the calculated dispersion curves in Figure 2. corresponds to an A0 phase velocity of 2560 m/s at room temperature. The angle of incidence is then calculated to be 7.7° by substituting the phase velocity and velocity of sound in air (344 m/s) in (2). 3D printed plastic wedges are used to accurately achieve this angle in practice. The transducers are not exposed to any high temperatures, due to their distance from the weld seam and the airgap insulating them from the workpiece.

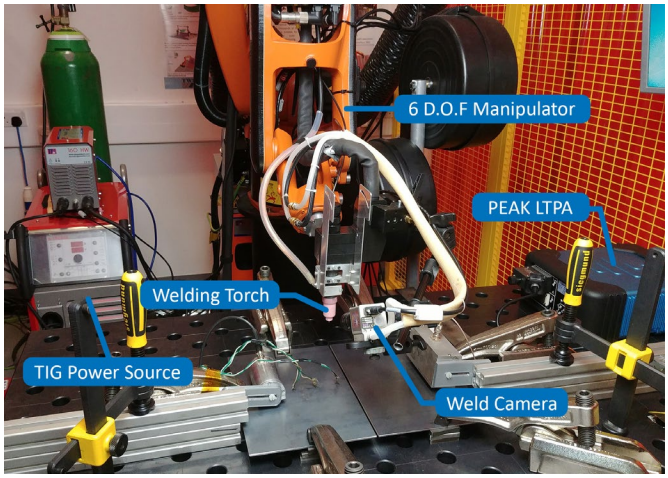

Fig. 4. Flexible welding and NDE cell showing TIG Power Source, Welding Torch, Weld Camera, 6 D.O.F Industrial Manipulator and PEAK LTPA phased array controller.

The transmitting transducer is excited through a 510 kHz 10 Cycle tone burst at a PRF of 200 Hz with a measured amplitude of 170 V. An A0 wave is excited in one plate with a travel direction perpendicular to the weld interface. As shown in Figure 1. a), the two plates are separated by a 3mm air gap and therefore prior to welding no guided waves can propagate across to the receiving transducer. Upon solidification of the weld joint however, the induced Lamb waves propagate through any subsequently welded joint and are received by the positionally aligned receiving transducer. The received signal amplitude when testing a reference plate of the same material and thickness is measured to be 200 μV, resulting in a total of 119 dB amplitude loss, which is lower than the expected 140 dB [15]. After reception by the second transducer, the signal is fed through two cascaded pre-amplifiers with hardware bandpass filters, giving a total of 200dB gain. Finally, the signal is digitised by a Peak NDT LTPA [31] low noise ultrasonic driver and acquisition system, using 128 averages. The averaging used by the acquisition system is cumulative, meaning that it returns one A-scan for every 128 samples it acquires, hence with the above configuration one sample is recorded every 0.64 seconds.

B. Equipment and Procedure

A JÄCKLE ProTIG 350 [32] power source and wire feeder unit and the GTAW process are used as illustrated in Figure 4. Automation of the welding process is provided through a KUKA KR5 Arc HW [33] 6 Degree Of Freedom robotic manipulator, externally controlled in real-time using the Robotic Sensor Interface (RSI) [34] at a 12ms interpolation cycle. Automatic voltage correction is used for closed loop adjustment of the welding torch offset. To measure the temperature gradient across the samples, three thermocouples are tack welded along the ultrasonic wave path at a distance of 20mm, 60mm and 100mm away from the weld seam respectively as per Figure 3. The thermocouples were positioned on one side of the weld only, making use of the symmetry of the workpiece and were found to have no measurable effect on the propagation of the guided waves. Relevant welding parameters and ultrasonic A-scans are recorded and encoded using the positional information of the manipulator-held welding torch. System control and data

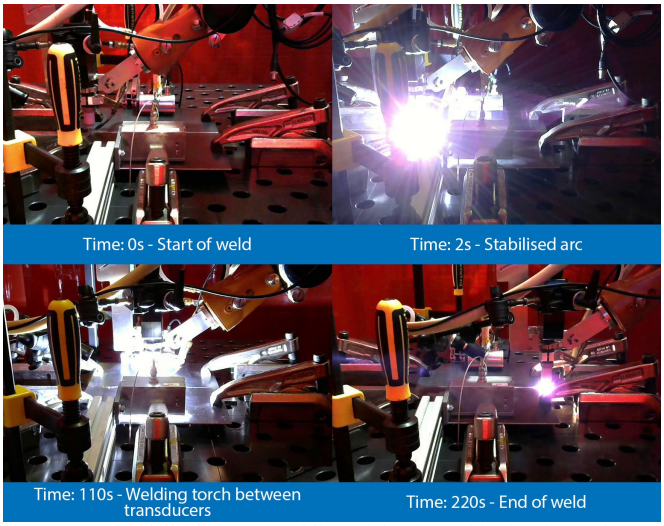

Fig. 5. Frames from video of welding trials: the welder is triggered at 0s; 110s later the welding torch passes through the middle of the inspection region; the weld is complete in 220s.

TABLE I
UNITS FOR MAGNETIC PROPERTIES

Sample	Current (A)	Voltage (V)	Travel Speed (mm/min)	Arc Energy (kJ/mm)	Wire Feed Rate (mm/min)
S1	66.5	12	80	0.59	1330
S2	76	12	80	0.68	1520
S3	85.5	12	80	0.77	1710
S4	90	12	80	0.81	1800
S5	95	12	80	0.86	1900
S6	104.5	12	80	0.94	2000
S7	114	12	80	1.03	2100

Welding parameters for welding trials S1 through S7. Wire feed rates were selected so that a stable weld pool could be developed in each sample. Arc energy values are calculated from (2).

logging is implemented using a National Instruments cRIO 9038 real-time embedded controller [35], programmed in the LabVIEW environment.

A 290mm butt weld is deposited between two 200x300x3 mm S275 Steel plates along their long side, while continuous in-process ultrasonic testing is performed, as demonstrated in the video frames in Figure 5. A sensitivity study was conducted with a total of 7 samples (S1-S7) , welded using varying levels of arc energy from 0.59 kJ/mm to 1.03 kJ/mm, shown in Table 1. Appropriate wire feed rates were selected so that a stable weld pool could be developed in each sample and the two plates could be connected with a weld bead. Values of arc energy under 0.59 kJ/mm were found to be too low to create a stable weld pool and values above 1.03 kJ/mm were found to result in weld burnthrough.

IV. SIGNAL PROCESSING

All signal processing is performed offline in MATLAB, and can be replicated and performed on-line through LabVIEW. A bandpass filter around the transducer's centre frequency (480kHz and 560kHz cut-off) in conjunction with a matched filter are used to remove noise from the environment and increase the system SNR. The maximum amplitude in the acquisition gate is recorded at each position of the welding torch and the resulting trace is denoised using a moving average of size 32 samples**.** Figure 6. shows the obtained

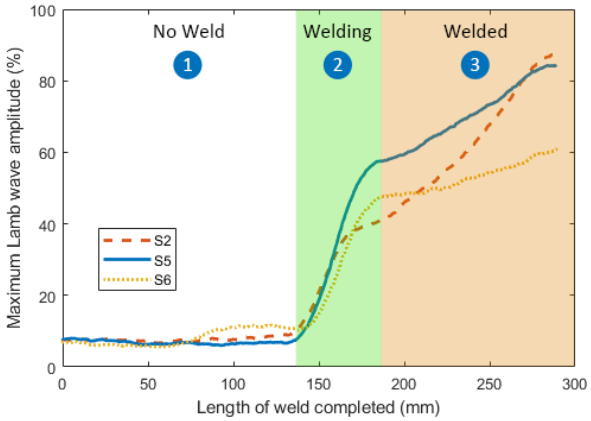

Fig. 6. Maximum recorded Lamb-wave amplitude vs length of weld completed for samples with low (blue), optimal (orange) and high (yellow) arc energy.

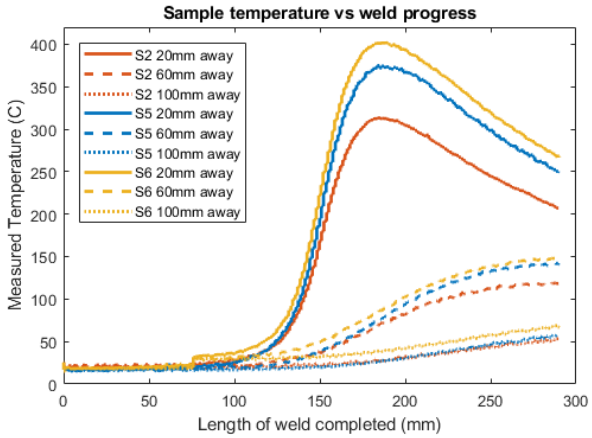

Fig. 7. Measured temperature at a distance of 20mm (solid), 60mm (dashed) and 100mm (dotted) away from the weld interface for samples with low (blue), optimal (green) and high (red) arc energy

curve for samples S2, S5 and S6 which were welded using low, optimal and high arc energy respectively. As mentioned in Section III the ultrasonic transducers are in a fixed position, therefore the x-axis of the plots corresponds to the length of weld seam completed at the time of measurement.

The low, optimal and high arc energy curves can be visually split into three regions as annotated in Figure 6. In region (1) only the background noise is observed at the receiver, as there is no weld present between the transducers and no guided waves could propagate across the gap. Region (2) resembles a Sigmoid (S shaped) curve with an approximate length of 50mm. This amplitude increase occurs when the welding torch is in the inspection region between the transducers at the time of measurement and corresponds to the solidification of the weld seam, as the Lamb waves cannot propagate through the liquid weld pool. Although the element size of the transducers is 30mm, the inspection region is expectedly widened due to beam spread. Authors have previously calculated, that for transducers with the same element size, located at a similar distance from the inspection point, the width of the Lamb wave beam would be approximately 50mm [36].

This phenomenon also explains the Sigmoid shape of the curve, as the sensitivity in both ends of the inspection window is reduced. The turning point in the curve at the end of region (2) occurs when the full weld in the inspection region is solidified. Any subsequent weld outside this region would not affect the amplitude of the ultrasonic wave, therefore this would be the point at which amplitude sizing should be carried out. However, the Lamb wave amplitude continues increasing at a steady rate in region (3). This can be explained by the sample cooling down and approaching the room temperature conditions for which the system is optimized. The temperature recorded by the thermocouples in Figure 7. confirms that this increase in amplitude is concurrent with the sample cooling down. The rate of change in region (3) also varies with the three samples, S2 with low arc energy has a higher slope than S5 and S6, as it cooled down quicker, and similarly S6 has a lower slope compared to S2 and S5 as it cooled down slower due to the higher arc energy used.

The dynamic nature of the welding process and the different levels of arc energy used for the samples rule out amplitude sizing, as the signal amplitude is greatly affected by temperature and in order for the conditions to stabilize, the sample needs to fully cool down to room temperature. Instead, we can take advantage of the fact that all measurements are taken in the same position and instead follow the evolution of the Lamb wave amplitude over time.

V. Results

The derivative of the Lamb wave amplitude with respect to time shown in Figure 8 reveals its maximum rate of change occurs when around 160mm of the weld has been completed. The peak of this derivative differs in the three samples S2, S5 and S6 by amplitude and location. Further destructive testing of the ultrasonically tested weld seam is performed in order to quantify and evaluate the weld quality and correlate this to the ultrasonic inspection results. Tensile specimen sections are waterjet cut from the weld seam in the inspection region directly between the two transducers and are put under tensile stress until failure. A second section measuring 40x20 mm is similarly cut from each sample for weld macrography and visual inspection. A weld macrograph is performed by cutting a cross section of a weld and then polishing and etching it using acid, in order to reveal the shape and size of the fused area.

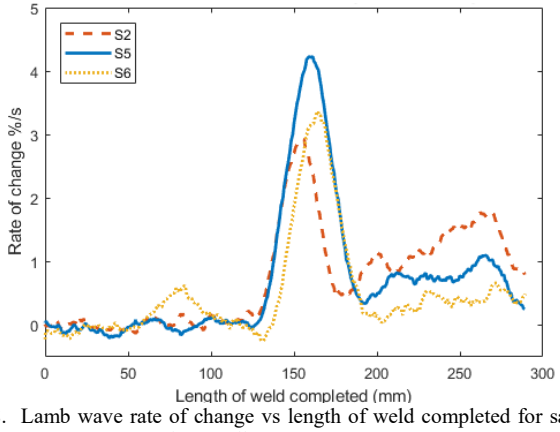

Fig. 8. Lamb wave rate of change vs length of weld completed for samples S2 (blue), S5 (orange) and S6 (yellow).

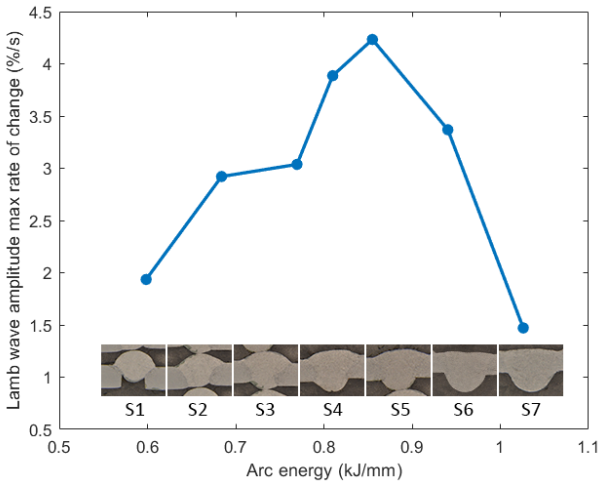

Fig. 9. Relationship between arc energy and Lamb wave amplitude peak rate of change. Macrographs of samples S1 through S7 are located under the corresponding datapoints on the graph.

The maximum Lamb wave amplitude rate of change for each sample is calculated and plotted against the arc energy used for the weld. Each point on the plot in Figure 9. corresponds to an individual sample, the macrograph of which is displayed underneath. The macrographs reveal that samples S1 and S2 observe a lack of root penetration due to the low arc energy used. On the other hand, samples S6 and S7 suffer from undercut and lack of weld crown due to the excessive arc energy used. The peak Lamb wave amplitude rate of change and the arc energy demonstrate a parabolic correlation, with the lack of penetration samples laying on the far left side of the plot, and the undercut samples laying on the far right. This is due to the geometry of the welds varying from the geometry of a continuous 3mm thick plate, resulting in the weld attenuating the Lamb waves.

The location of the peak Lamb wave rate of change for each sample is also measured and plotted vs the arc energy. As samples S1 and S7 ae at the extreme levels of arc energy, the differential plots do not contain a clear peak and are therefore excluded from the graph. Figure 10. shows that the location of the peak Lamb wave rate of change varies linearly with arc energy, therefore this measure could be used to predict if the arc energy used for the weld section was insufficient or excessive.

Results from tensile stress testing to failure in Figure 11 confirm that the two samples with identified lack of root penetration have a lower failure point, compared to the rest of the samples. The samples with high arc energy however do not show a reduction in tensile strength. Although this is true at the time of manufacture, excessive welding power and undercut can lead to cracking of the weld when the components are exposed to fatigue loading [37].

The temperature of the workpiece has a strong adverse effect on the propagation of the Lamb waves due to the change in speed of sound. As the transducers are static and are set at an angle for optimal transmission at room temperature, any heat introduced into the sample reduces the amount of energy inserted into the workpiece. Nevertheless, the proposed technique was found to be sensitive to changes in arc energy in the butt welded mild steel samples. By setting an adequate threshold for the peak Lamb wave rate of change and

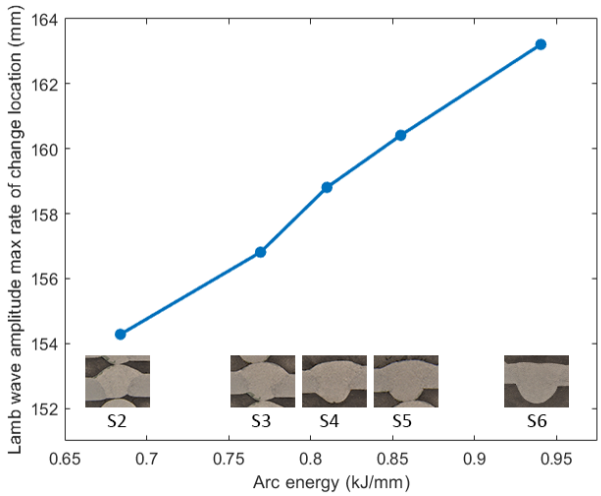

Fig. 10. Relationship between arc energy and Lamb wave amplitude peak rate of change location. Samples S1 and S7 at both extremes were excluded as they were outliers in the plot.

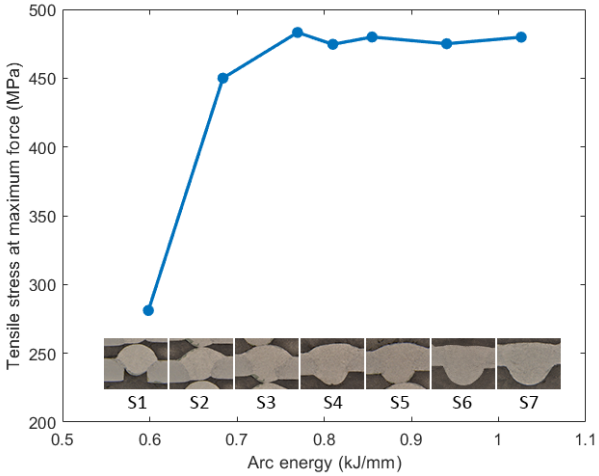

Fig. 11. Relationship between arc energy and maximum tensile stress at failure for samples S1 through S7. A decrease in tensile strength is observed in the samples with insufficient arc energy- S1 and S2

measuring the location of this peak, the demonstrated approach can indeed be used to predict whether lack of root penetration or undercut can be expected in the produced weld. The lack of couplant required for the air-coupled ultrasonic transmission provides a non-obtrusive method for in-process screening of the welded joint. Therefore, this method could be used to provide an early indication of flaws developing in the weld and can be used in-situ for process control.

VI. Future Work

Despite the low signal amplitudes involved, the main limitation of the outlined approach was the fixed location of the ultrasonic transducers, as only a small section of the welded joint was inspected. A more practical application of the UT method would involve transversal scanning the transducers along with the welding torch. The obtained ultrasonic B-scan would consist of multiple measurements and would represent a complete image of the weld seam. In an industrial environment, the welding parameters and arc energy used for all components would be the same and, therefore, the temperature and cooling rate would not change from sample to sample. This, along with maintaining the same distance from

the welding torch for all ultrasonic measurements, would remove the workpiece temperature as a variable. Contrary to the expectations, transducer misalignment was not the primary factor that influenced the amplitude of the Lamb waves. The exact effects of the high temperature inspection region should be further investigated using FEA simulations. A sensitivity study should also be carried out using realistic artificially induced defects including cracks, porosity and lack of fusion, in order to determine the probability of detection for each type of defect, which in turn would identify suitable applications for the proposed approach.

VII. Conclusion

An in-process non-destructive testing procedure using air-coupled ultrasonic transducers was outlined and demonstrated. A total of seven butt welded mild steel samples with varying levels penetration between 0.59 kJ/mm to 1.03 kJ/mm were inspected and the results were analysed. The effects of temperature on the amplitude of guided Lamb waves was outlined and demonstrated through ultrasonic measurements of a section of the welded joints.

The rate of change of the Lamb wave amplitude was found to be correlated with the specific arc energy used in each sample. The location and the amplitude of the peak Lamb wave rate of change can be used to determine if the final weld would exhibit lack of root penetration or undercut.

Future work includes scanning the full length of the weld and optimising the parameters for the specific thermal gradient of the hot sample in order to maximise the transmission efficiency of the ultrasonic waves. Further studies including realistic defects would aid to identify suitable practical applications for the proposed approach.

References

[1] R. J. Ditchburn, S. K. Burke, and C. M. Scala, "NDT of welds: state of the art," *NDT E Int.*, vol. 29, no. 2, pp. 111–117, Apr. 1996.

[2] Germany Trade & Invest, "GTAI - Industrie 4.0 – What is it?," *Germany Trade & Invest*. [Online]. Available: https://www.gtai.de/GTAI/Navigation/EN/Invest/Industries/Industrie-4-0/Industrie-4-0/industrie-4-0-what-is-it.html#1798424. [Accessed: 02-Sep-2019].

[3] C. Mineo *et al.*, "Fast ultrasonic phased array inspection of complex geometries delivered through robotic manipulators and high speed data acquisition instrumentation," in *2016 IEEE International Ultrasonics Symposium (IUS)*, 2016, pp. 1–4.

[4] High Value Manufacturing Catapult, "AMRC's robot research cuts cost of producing aircraft," 03-Dec-2018. [Online]. Available: https://hvm.catapult.org.uk/case-study/ncc-helps-dymag-re-invent-the-wheel/. [Accessed: 05-Sep-2019].

[5] J. F. Lancaster, "The physics of fusion welding. Part 1: The electric arc in welding," *IEE Proc. B - Electr. Power Appl.*, vol. 134, no. 5, pp. 233–254, Sep. 1987.

[6] A. Salminen, H. Piili, and T. Purtonen, "The characteristics of high power fibre laser welding," *Proc. Inst. Mech. Eng. Part C J. Mech. Eng. Sci.*, vol. 224, no. 5, pp. 1019–1029, May 2010.

[7] K. Weman, *Welding Process Handbook*, Second. Woodhead Publishing Limited, 2012.

[8] "What is the difference between heat input and arc energy?" [Online]. Available: twi-global.com/technical-knowledge/faqs/faq-what-is-the-difference-between-heat-input-and-arc-energy.aspx. [Accessed: 04-Sep-2019].

[9] W. J. Fleming, "New Automotive Sensors—A Review," *IEEE Sens. J.*, vol. 8, no. 11, pp. 1900–1921, Nov. 2008.

[10] A. Carullo and M. Parvis, "An ultrasonic sensor for distance measurement in automotive applications," *IEEE Sens. J.*, vol. 1, no. 2, pp. 143-, Aug. 2001.

[11] J. Mirapeix Serrano, R. Ruiz-Lombera, J. J. Valdiande, A. Cobo, and J. M. Lopez-Higuera, "Colorimetric Analysis for On-Line Arc-Welding Diagnostics by Means of Plasma Optical Spectroscopy," *IEEE Sens. J.*, vol. 16, no. 10, pp. 3465–3471, May 2016.

[12] T. Font comas, C. Diao, J. Ding, S. Williams, and Y. Zhao, "A Passive Imaging System for Geometry Measurement for the Plasma Arc Welding Process," *IEEE Trans. Ind. Electron.*, vol. 64, no. 9, pp. 7201–7209, Sep. 2017.

[13] J. Liu, Z. Fan, S. I. Olsen, K. H. Christensen, and J. K. Kristensen, "Boosting Active Contours for Weld Pool Visual Tracking in Automatic Arc Welding," *IEEE Trans. Autom. Sci. Eng.*, vol. 14, no. 2, pp. 1096–1108, Apr. 2017.

[14] H. Gao, B. Lopez, X. Minguez, and J. Chen, "Ultrasonic inspection of partially completed welds using EMAT-generated surface wave technology," in *NDT New Technology & Application Forum (FENDT), 2015 IEEE Far East*, 2015, pp. 263–266.

[15] S. P. Kelly, R. Farlow, and G. Hayward, "Applications of through-air ultrasound for rapid NDE scanning in the aerospace industry," *IEEE Trans. Ultrason. Ferroelectr. Freq. Control*, vol. 43, no. 4, pp. 581–591, Jul. 1996.

[16] "Ultrasonic phased array wedge for inspecting high-temperature parts up to 150°C." [Online]. Available: https://www.olympus-ims.com/en/applications/ultrasonic-phased-array-wedge-for-inspecting-high-temperature-parts-up-to-150c/. [Accessed: 02-Sep-2019].

[17] J. Ji, W. Chen, and X. Yang, "Arc welding inverter with embedded Digital Active EMI controller," in *2016 IEEE Applied Power Electronics Conference and Exposition (APEC)*, 2016, pp. 493–498.

[18] S. E. Burrows, B. Dutton, and S. Dixon, "Laser generation of lamb waves for defect detection: Experimental methods and finite element modeling," *IEEE Trans. Ultrason. Ferroelectr. Freq. Control*, vol. 59, no. 1, pp. 82–89, Jan. 2012.

[19] D. Cerniglia and N. Montinaro, "Defect Detection in Additively Manufactured Components: Laser Ultrasound and Laser Thermography Comparison," *Procedia Struct. Integr.*, vol. 8, pp. 154–162, Jan. 2018.

[20] L. Zeng and J. Lin, "Structural damage imaging approaches based on lamb waves: A review," in *2011 International Conference on Quality, Reliability, Risk, Maintenance, and Safety Engineering*, 2011, pp. 986–993.

[21] F. Gao, L. Zeng, J. Lin, and Y. Shao, "Damage assessment in composite laminates via broadband Lamb wave," *Ultrasonics*, vol. 86, pp. 49–58, May 2018.

[22] P. Huthwaite and M. Seher, "Robust helical path separation for thickness mapping of pipes by guided wave tomography," *IEEE Trans. Ultrason. Ferroelectr. Freq. Control*, vol. 62, no. 5, pp. 927–938, May 2015.

[23] F. Simonetti and M. Y. Alqaradawi, "Guided ultrasonic wave tomography of a pipe bend exposed to environmental conditions: A long-term monitoring experiment," *NDT E Int.*, vol. 105, pp. 1–10, Jul. 2019.

[24] J. Zhang, H. Ma, W. Yan, and Z. Li, "Defect detection and location in switch rails by acoustic emission and Lamb wave analysis: A feasibility study," *Appl. Acoust.*, vol. 105, pp. 67–74, Apr. 2016.

[25] G. Dobie, R. Summan, S. G. Pierce, W. Galbraith, and G. Hayward, "A Noncontact Ultrasonic Platform for Structural Inspection," *IEEE Sens. J.*, vol. 11, no. 10, pp. 2458–2468, Oct. 2011.

[26] G. Dobie, "Ultrasonic Sensor Platforms for Non-Destructive Evaluation," p. 308.

[27] B. Pavlakovic, M. Lowe, O. Alleyne, and P. Cawley, "Disperse: a general purpose program for creating dispersion curves. Review of progress in quantitative nondestructive evaluation," *Rev. Prog. Quant. Nondestruct. Eval.*, vol. 16A, 1997.

[28] C. B. Scruby and B. C. Moss, "Non-contact ultrasonic measurements on steel at elevated temperatures," *NDT E Int.*, vol. 26, no. 4, pp. 177–188, Aug. 1993.

[29] A. Gachagan, G. Hayward, S. P. Kelly, and W. Galbraith, "Characterization of air-coupled transducers," *IEEE Trans. Ultrason. Ferroelectr. Freq. Control*, vol. 43, no. 4, pp. 678–689, Jul. 1996.

[30] S. P. Kelly, G. Hayward, and T. E. Gomez, "An air-coupled ultrasonic matching layer employing half wavelength cavity resonance," in *2001*

IEEE Ultrasonics Symposium. Proceedings. An International Symposium (Cat. No.01CH37263), 2001, vol. 2, pp. 965–968 vol.2.
[31] "PEAK LTPA Specification," *PeakNDT*. [Online]. Available: https://www.peakndt.com/products/ltpa/. [Accessed: 05-Sep-2019].
[32] Jäckle Schweiß- und Schneidtechnik GmbH, "Jackle ProTIG 350AC / DC Operating Manual." .
[33] KUKA Robot Group, "KR 5 arc HW, KR 5 arc HW-2 Specification." 23-Mar-2016.
[34] "KUKA.RobotSensorInterface," Apr-2014. [Online]. Available: http://www.kuka-robotics.com.
[35] "cRIO-9038 - National Instruments." [Online]. Available: http://www.ni.com/en-gb/support/model.crio-9038.html. [Accessed: 05-Sep-2019].
[36] G. Dobie, S. Gareth Pierce, and G. Hayward, "The feasibility of synthetic aperture guided wave imaging to a mobile sensor platform," *NDT E Int.*, vol. 58, pp. 10–17, Sep. 2013.
[37] C. Steimbreger and M. D. Chapetti, "Fatigue strength assessment of butt-welded joints with undercuts," *Int. J. Fatigue*, vol. 105, pp. 296–304, Dec. 2017.

Momchil Vasilev was born in Sofia, Bulgaria in 1994. He received a BEng with Honours in electronic & electrical engineering from the University of Strathclyde, Glasgow, in 2017.
From 2016 to 2017 he was a part time researcher at the Centre for Ultrasonic Engineering (CUE) in the University of Strathclyde and in 2017 he joined the group as a PhD researcher. His interests include non-destructive evaluation, in-process ultrasonic inspection of welds and sensor enabled robotic welding.

Charles N. MacLeod received the master's degree (With Distinction) in electrical and mechanical engineering from the University of Strathclyde. He received the Ph.D. degree in Automated Non-Destructive Evaluation and is currently a Lecturer with the Centre for Ultrasonic Engineering, University of Strathclyde leading In-Process Inspection activities. He has over 15 years experience in in Automated Non- Destructive Evaluation areas such as robotics and ultrasonic sensors. He was a recipient of the prestigious University of Strathclyde EPSRC Doctoral Prize in 2014, for his work investigating automated NDE for high-value manufacturing of composites

Walter Galbraith received the B.A. degree and the M.Phil. degree for work on hydrophones from the Open University, Milton Keynes, U.K., in 1986 and the University of Strathclyde, Glasgow, U.K., in 1997.,He is an Experimental Officer within the Centre for Ultrasonic Engineering, University of Strathclyde. After completing a marine engineering apprenticeship at Upper Clyde Shipbuilders, he joined the Electronics Group in the Metallurgy Department of the University of Strathclyde, where he was primarily involved with mass spectroscopy and other analytical instrumentation techniques. His research interests include the development of ultrasonic air coupled transducers, power ultrasound and micromachining techniques for transducer fabrication.

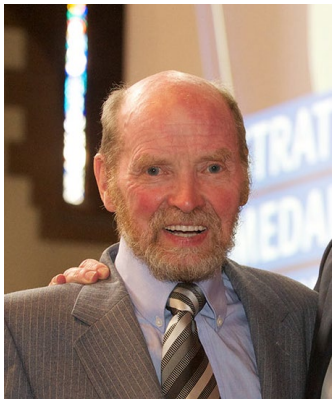

Yashar Javadi is a postdoctoral research associate at the University of Strathclyde. He has BSc (2004), MSc (2008) and PhD (2013) in mechanical engineering. In a career spanning over 15 years in the field of manufacturing engineering (particular focus on welding, NDT, additive manufacturing and robotics), he has worked as a postdoctoral research associate (at The University of Manchester and the University of Strathclyde), lecturer, manager of the welding/NDT department and welding engineer. He has published 59 refereed technical articles (including 32 journal papers), first author on 41 papers, and he has reviewed >118 manuscripts for many engineering journals (including IEEE journals). Currently, he is a member of Centre for Ultrasonic Engineering (CUE), at the University of Strathclyde, where he is involved in the in-process inspection of the welding and Wire + Arc Additive Manufacturing (WAAM).

Euan Foster is a current engineering doctorate (EngD) student at the University of Strathclyde, via the Research Centre for Non Destructive Evaluation in the UK. His research interests include ultrasonic feature guided wave and bulk wave inspection of nuclear assets and resistance seam welds, as well as data fusion between different non-destructive testing techniques. Euan has a MEng in Aero-Mechanical engineering, and has previously worked as an opto-mechanical engineer at Thales UK. During his undergraduate degree, Euan has also worked at the biomedicial start up, Channel Medsystems, in SF USA, and has completed two summers of research within the Mechanical and Aerospace department at the University of Strathclyde.

Dr Gordon Dobie is a Senior Lecturer in Electronic & Electrical Engineering at the University of Strathclyde, UK. He has 12 years' experience and almost 60 publications in automation, structural inspection, sensors and signal processing. Dr Dobie has a strong track record in industrial engagement working with partners in the Oil and Gas, Nuclear and Healthcare sectors to deliver novel solutions to real industrial problems. His work led directly to an onsite robotic inspection of a critical path reprocessing vessel at Sellafield. Dr Dobie has licensed key parts of his team's mobile robotics technology to SME members of the Research Centre for Non-Destructive Evaluation. He currently leads a team of 12 PhD/EngD students and postdoctoral researchers.

S. Gareth Pierce is based in the Centre for Ultrasonic Engineering (CUE) at The University of Strathclyde. With a background in Applied Physics and Engineering, his research interests include robotic systems for Non-Destructive Testing & Evaluation (NDT&E), ultrasonics and acoustics, structural health monitoring, applied optics, instrumentation and machine learning. He is EU Robotics member for the UK Research Centre in Non-Destructive Testing (RCNDE), member of the Association for Robots in Architecture, and Technical Committee member for the European Workshop on Structural Health Monitoring.

Anthony Gachagan (M'04) received the Ph.D. degree from the University of Strathclyde, Glasgow, U.K., in 1996, focusing on the development of air-coupled piezoelectric transducer technology and has continued to develop his ultrasonic transduction research into array technology and high power system. He is currently a Professor with the Department of Electrical and Electronic Engineering, Strathclyde University, where he is also the Director of the Centre for Ultrasonic Engineering. He focused on the field of ultrasound for over 25 years. He has authored or co-authored over 120 research publications across a broad application range including non-destructive evaluation, sonar, bioacoustics, and industrial process control. His research interests encompass ultrasonic transducers and arrays, array imaging processing, power ultrasound, industrial process control instrumentation, and the application of coded excitation techniques.